6. SITE 557[1]

Shipboard Scientific Party[2]

HOLE 557

Date occupied: 29 September, 2119 hr.

Date departed: 30 September, 2300 hr.

Time on hole: 25.7 hr.

Position (latitude; longitude): 38°49.95′N; 32°33.58′W

Water depth (sea level; corrected m, echo-sounding): 2143

Water depth (rig floor; corrected m, echo-sounding): 2153

Bottom felt (m, drill pipe): 2155

Penetration (m): 463.5

Number of cores: 1

Total length of cored section (m): 3

Total core recovered (m): 1.2

Core recovery (%): 40

Oldest sediment cored:
Depth sub-bottom (m): 460.5
Nature: Volcaniclastic nannofossil chalk
Age: late Miocene
Measured velocity (km/s): 1.76

Basement:
Depth sub-bottom (m): 460.5
Nature: Basalt

Principal results: Because of the depleted character of the oceanic crust found unexpectedly at Site 556 (MAR-2), we decided to drill at least one additional hole closer to the ridge on the same flow line passing through the Azores Triple Junction (Fig. 1). Hole 557 (MAR-1) is located on Magnetic Anomaly 5D (18 Ma) in the center of a broad (40-km wide) elevated basin. This site is roughly on the same isochron as Site 335 drilled during Leg 37 on a flow line passing through the FAMOUS area (Aumento, Nelson, et al., 1977).

After washing down through 460.5 m of sediments and coring 3 m of basalts, we abandoned the hole because of an approaching storm. The recovered samples are fresh and are characterized by high iron and titanium contents and low magnesium content; the concentrations of magmaphile elements (Nb = 30 ppm, Zr = 220 ppm, Ti = 21,100 ppm, V = 420 ppm) display an "enriched" normalized diagram typical of the basalts associated with the present-day Azores Mantle Plume. In conjunction with the new results at Site 556, the present findings demonstrate that the effect of the mantle plume at the Azores Triple Junction changed radically between 34 and 18 Ma.

For this site, the following analyses were not done: sediment accumulation rates, pore water chemistry, and downhole measurements.

OPERATIONS

Approach to Site

The criteria for selecting Site 557 were that it should be on roughly the same isochron as Site 335 (i.e., 16 Ma) and on the same flow line as Site 556 (i.e., north of the Pico Fracture Zone). A tentative location was determined from the magnetic and seismic profiler records made on the *Glomar Challenger* enroute to Site 556 (Fig. 2). The site chosen was on Anomaly 5D, with a water depth of about 2150 m, in the center of a broad (40-km wide) elevated basin that is bounded by ridges to the west and east. The seismic profile indicated 0.4 s of sediments above a strong acoustic basement reflector (Fig. 3).

The site was approached by steaming eastward from Site 556 along a track 10 n. mi. north of the earlier *Glomar Challenger* track. At the estimated longitude of the site, we changed course to 180° in order to make a perpendicular crossing of the site. A satellite fix along this southward course indicated that we were slightly east of the site, and a final course correction to 240° was made that brought us across the site at 2119Z 29 September, at which time the beacon was dropped. Seismic data were collected for an additional 3 n. mi. on a course of 180° to check for unexpected basement features south of the site. The underway geophysical gear was then retrieved and the site was occupied at 2300Z.

On-Site Operations

Our only objective at this site was to recover representative basement samples. With this limited objective in mind, it was decided to proceed with drilling operations despite the fact that Hurricane Irene was on a track that would take her close to the site in roughly 30 hr. No mudline core was taken, and sediments were washed down to a depth of 425 m sub-button, at which time wash Core H1 was taken to replace the core barrel. Basement was felt at a sub-bottom depth of 460 m and was cored for approximately 1 hr. At 1730Z, drilling operations were stopped in the face of deteriorating weather conditions and the drill string was recovered (Table 1). Wash Core H2 and Core 1 were removed from the core barrel when the last section of pipe was brought aboard at 2216Z.

---

[1] Bougault, H., Cande, S. C., et al., *Init. Repts. DSDP*, 82: Washington (U.S. Govt. Printing Office).

[2] Henri Bougault (Co-Chief Scientist), IFREMER (formerly CNEXO), Centre de Brest, B. P. 337, 29273 Brest Cedex, France; Steven C. Cande (Co-Chief Scientist), Lamont-Doherty Geological Observatory, Columbia University, Palisades, New York; Joyce Brannon, Department of Earth and Planetary Sciences, Washington University, St. Louis, Missouri; David M. Christie, Hawaii Institute of Geophysics, University of Hawaii at Manoa, Honolulu, Hawaii; Marlene Clark, Department of Geology, Florida State University, Tallahassee, Florida; Doris M. Curtis, Curtis and Echols, Geological Consultants, Houston, Texas; Natalie Drake, Department of Geology, University of Massachusetts, Amherst, Massachusetts; Dorothy Echols, Department of Earth and Planetary Sciences, Washington University, St. Louis, Missouri (present address: Curtis and Echols, Geological Consultants, 800 Anderson, Houston, Texas 77401); Ian Ashley Hill, Department of Geology, University of Leicester, Leicester LEI 7RH, United Kingdom; M. Javed Khan, Lamont-Doherty Geological Observatory, Columbia University, Palisades, New York (present address: Department of Geology, Peshawar University, Peshawar, Pakistan); William Mills, Deep Sea Drilling Project, Scripps Institution of Oceanography, La Jolla, California (present address: Ocean Drilling Program, Texas A&M University, College Station, Texas 77843); Rolf Neuser, Institut für Geologie, Ruhr Universität Bochum, 4630 Bochum 1, Federal Republic of Germany; Marion Rideout, Graduate School of Oceanography, University of Rhode Island, Kingston, Rhode Island (present address: Department of Geology, Rice University, P. O. Box 1892, Houston, Texas 77251); and Barry L. Weaver, Department of Geology, University of Leicester, Leicester, LEI 7RH, United Kingdom (present address: School of Geology and Geophysics, University of Oklahoma, Norman, Oklahoma 73019).

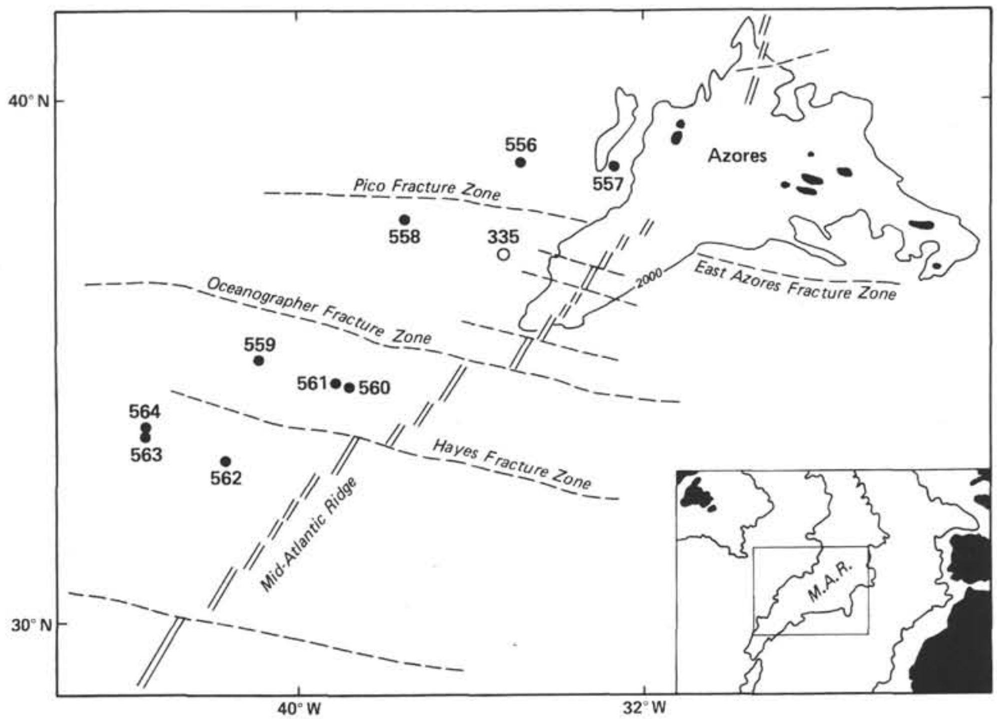

Figure 1. Site location map, Leg 82.

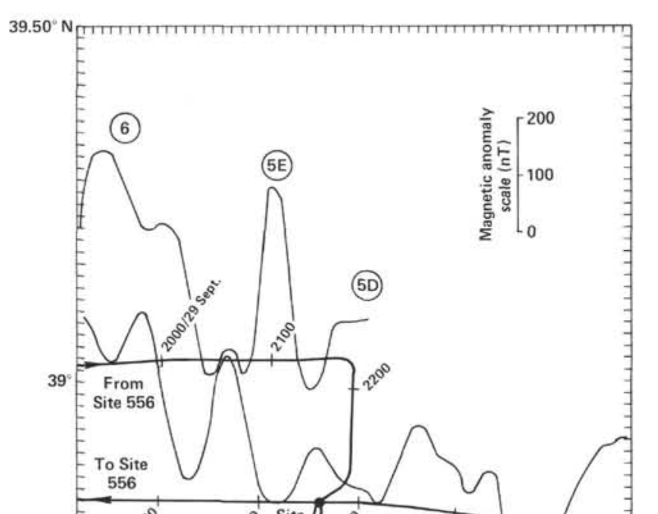

Figure 2. Approach and site survey tracks for Site 557. Heavy line is the ship's track with hours marked in GMT. Faint line is the magnetic anomaly line, projected perpendicularly from ship's track. Circled numbers are anomalies based on work at Lamont-Doherty Geological Observatory.

SEDIMENT LITHOLOGY

Hole 557 was washed from a sub-bottom depth of about 2150 m down through 460.5 m of sediments where the drill encountered basalt. Two wash cores were recovered. Because of the nature of the wash core (Core H1), we cannot assign an upper limit to the age range of the sediments at this site, nor can we evaluate the significance of several interesting details observed in the recovered sediments. The oldest sediments in Core H2 are dated at 10 to 12 Ma by foraminifers.

On visual description, the recovered material in Core H1 is nannofossil to foraminiferal-nannofossil chalk and limestone, whereas the sedimentary rock in Core H2 consists of alternating dark to light mudstones to limestones in distal turbidite cycles. However, the presence of microlaminae and grading in Core H1 suggest that the limestones and chalks are a distal, dwindling continuation of the deposition represented by Core H2. Therefore we recognize in the recovered cores only one sediment unit divided into "a" and "b" subunits (see Table 2).

Subunit 1a

Subunit 1a (0–425.5 m) (Section 557-H1-1 through 557-H1-2, 35 cm and H1, CC) includes 220 cm of white to greenish gray (2.5YN 7 to 2.5YN 4, 5YN 8, and 5G 7/1) nannofossil chalk to limestone and foraminiferal-nannofossil chalk of the late Miocene (5.2 to 10 Ma). Although much of the core is brecciated by drilling, enough undisturbed material remains to preserve the sedimentary structures. These include parallel and wavy laminae and occasional micro-crosslaminae, alternating with unbedded, bioturbated layers. Thin-section examination shows that the laminated layers represent "mi-

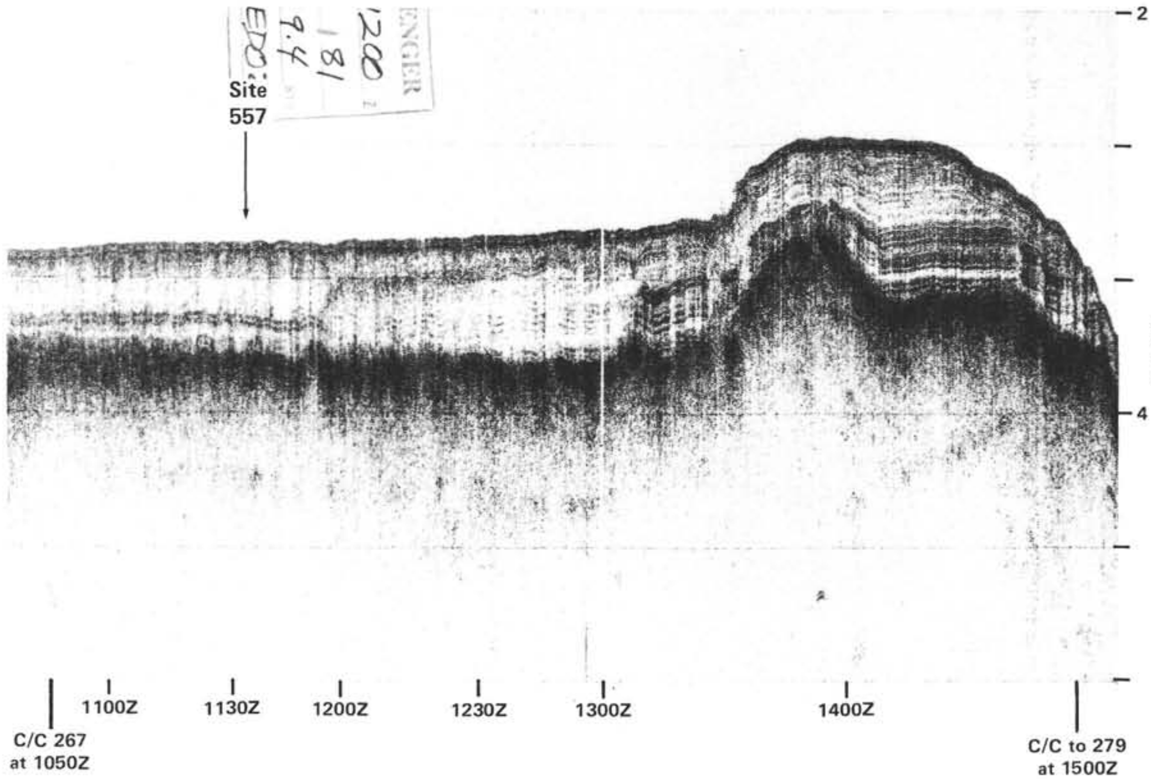

Figure 3. *Glomar Challenger* seismic record crossing to Site 557 made on route to Site 556. C/C is course change. For location of profile, see Figure 2.

Table 1. Coring summary, Hole 557.

Core	Date (Sept. 1981)	Time	Depth from drill floor (m)	Depth below seafloor (m)	Length cored (m)	Length recovered (m)	Percent recovered
H1	30	1442	2155.0–2580.5	0.0–425.5	0.0	0.00	0
H2	30	2216	2580.5–2615.5	425.5–460.5	0.0	0.00	0
1	30	2216	2615.5–2618.5	460.5–463.5	3.0	1.20	40
					3.0	1.20	40

cro-turbidite" sequences a few millimeters thick, grading upward from chalk with less abundant small foraminifers to chalk with more abundant, smaller foraminifers, forming a foraminiferal ooze at the bedding plane contact with the overlying lamina. The bioturbated portions contain a greater proportion of nannofossils. The slightly darker layers appear to be more siliceous than the lighter ones.

Several interesting details appear in this unit but, because of the possible displacement by washing, we cannot make a meaningful interpretation of their significance.

1. A cobble-size fragment of fresh vesicular basalt, about 6 mm in diameter, was embedded in the sediment in C H1,CC. It looks like a volcanic bomb, but there is little evidence of pyroclastic material elsewhere in the unit, except for a small quantity of fresh ash in 557-H1-1, 104 cm. The sediment layers immediately adjacent to the basalt fragment are chertified and appear to be de-

Table 2. Sediment lithology summary, Hole 557.

Core	Lithologic unit	Depth and thickness (m)	Main colors	Main lithology	Main components	Structure	Age
H1	1a	0 m washed to 425.5 m	Light gray to greenish gray	Nannofossil chalk, foraminiferal-nannofossil chalk, and limestone	Nannofossils foraminifers, and siliceous fossils	Parallel, wavy, and crosslaminae cyclic with bioturbated intervals	late Miocene
H2	1b	425.5–460.5	Alternating dark to light greenish gray	Cyclic foraminiferal-nannofossil limestone with calcareous volcaniclastic mudstone	Nannofossils foraminifers, and volcaniclastic mud	Graded cycles, parallel, wavy laminae and crosslaminae	early late Miocene

Note: Core 557-1 is not included in this table because it consisted of only basalt.

formed parallel with the fragment outline, but we do not know the true orientation of the fragment in the core.

2. Pieces of chert, about 4–5 cm wide and 2–3 cm thick, interbedded with limestone, were found in 557-H1-1, 28–32 cm and in 557-H1,CC. The chert contains abundant silicified foraminifers and includes small patches of unreplaced carbonate. One of the pieces has faint parallel and wavy laminations and micro-crosslaminae. The other has contorted swirls of interlayered limestone and chert.

3. A hard, encrusting, nodular "celestone," composed predominantly of foraminiferal chalk, calcite, and celestite, was found in 557-H1-1, 0–8 cm, in association with drill-brecciated foraminiferal-nannofossil chalk. We verified the optical identification of the celestite by X-ray diffraction (XRD) and X-ray fluorescence (XRF) (for strontium) analyses. The celestite is crystallized in optically continuous patches so that the entire thin section, in polarized light, presents a mosaic effect.

Subunit 1b

Subunit 1b (425.5–460.5 m) (557-H2-1 through 557-H2-7) includes 9.5 m of light greenish gray and light gray (5G 4/1 to 5GY 7/1) to dark greenish gray (5G 2/1) and black limestone and nannofossil limestone, volcaniclastic nannofossil limestone, and calcareous volcaniclastic mudstone of the early late Miocene (10 to 12 Ma). There appears to be almost no drilling disturbance in this relatively well-lithified unit. The dark and light sediments occur in cyclic pairs, beginning with dark mudstone at the base of each cycle (see Fig. 4), in sharp contact with the underlying limestone, and grading upward into lighter-colored volcaniclastic nannofossil limestone and limestone. Not all cycles are complete, and some include only the mudstone and volcaniclastic nannofossil limestone. The incomplete cycles, however, appear to be subcycles within larger cycles. The larger cycles are 1–1.5 m thick; the smaller subcycles are 10–30 cm thick. We interpret these sediments as distal turbidites derived from a volcanic ridge or island.

The darker portions of the sequence exhibit graded bedding, in fining-upward cycles from mudstone with 25–40% silt-size components to limestone with 10–20% silt-size components, then to almost pure biogenic limestone. Parallel and wavy laminations occur in the darkest portion of the turbidite cycles. Bioturbation occurs only in the light-colored portion. In many cases, borings are truncated by the sharp contact with the overlying black sediment.

Carbonate content is distinctly different in each of the three dominant lithologic categories making up the turbidite cycles. In the sections in which carbonate bomb measurements were made, the lowest carbonate percentages are in the darkest lithology, where the carbonate percentage range is 10–14%. The major components of these samples are volcaniclastic material, including ash and lithic fragments, clay derived from alteration of such material, foraminifers, and nannofossils. Opaque minerals are also prominent.

In the medium-colored, greenish gray parts of the cycles, or in laminae or beds within the lighter or darker por-

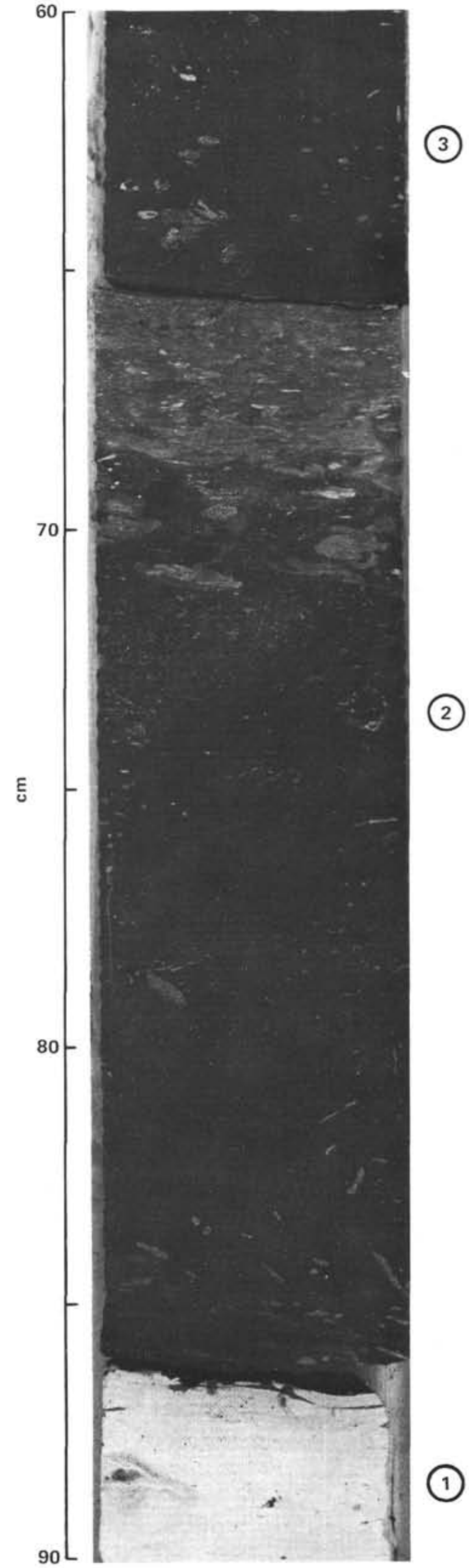

Figure 4. Photo of 557-H2-4, 60-90 cm. Portions of three turbidite cycles: (1) white limestone at the top of cycle; (2) black calcareous volcaniclastic mudstone grading up into gray volcaniclastic limestone; (3) black calcareous volcaniclastic mudstone.

tions, the carbonate content ranges up to 45%. In these layers, the dominant components are nannofossils, foraminifers, volcaniclastic material, and clay.

The light-colored limestone portions of the cycles are composed of 78–88% carbonate. The dominant components are nannofossils and foraminifers.

BIOSTRATIGRAPHY

Material recovered from the two sediment cores drilled at Site 557 is from the late Miocene (5.2–12 Ma). The dates are tentatively based on foraminifers. Nannofossils are poorly preserved and not definitive in this interval.

Nannofossils

Because of poor preservation of calcareous nannofossils, the sediments at Site 557 cannot be precisely zoned using this fossil group. In 557-H1,CC *Calcidiscus macintyrei* and *Reticulofenestra pseudoumbilica* are abundant. Discoasters from these two samples are rare and cannot be identified to the species level. The assemblage suggests an assignment of middle Miocene to lower Pliocene.

Rare *Discoaster variabilis* (in addition to *C. macintyrei, R. pseudoumbilica*, and *Sphenolithus abies*) are contained in 557-H2-3, 77 cm and 557-H2-6, 53 cm. A possible *berggrenii* is found in 557-H2-3, 77 cm. Because of poor preservation, a middle Miocene to lower Pliocene is the best assignment that can be made from these samples.

The middle Miocene to lower Pliocene assignment suggested by the calcareous nannofossils for these sediments is contrary to the upper Miocene assignment indicated by the planktonic foraminifers.

Foraminifers

The core catcher of Core H1, drilled to 425.5 m at Site 557, contains an upper Miocene, white chalkly marl. Foraminifers are common to abundant, and preservation is moderate to good. The assemblage consists of abundant *Globorotalia conoidea, Globigerina nepenthes* and an accompanying fauna of *Globorotalia plesiotumida, G. conomiozea, Globigerinoides quadrilobatus triloba, Sphaeroidinellopsis subdehiscens*, and *Orbulina universa*. Well-preserved benthic forms are present and the environment is interpreted as warm temperate. Figure 5 shows the tentative placement within the numeric time scale of this sample and the other samples examined from this hole.

Foraminifers recovered from 557-H1-1, 13–15 cm are characteristic of the uppermost upper Miocene foraminiferal Zone N17 (5.2–7.8 Ma).

The washed residue from a piece of chert in 557-H1-1, 33–35 cm, which was in contact with a pale green-gray carbonate, contained many tiny foraminifers and a normal-size upper Miocene fauna.

An upper Miocene foraminiferal fauna (probably Zone N17) is contained in 557-H1-1, 103–105 cm. Sections 557-H2-1 and 557-H2-3 are also Miocene; the fauna in samples from Sections 557-H2-6 and 557-H2-7 indicate a lower upper Miocene assignment (10.5–12 Ma; Zones N15–N14) (see Fig. 5).

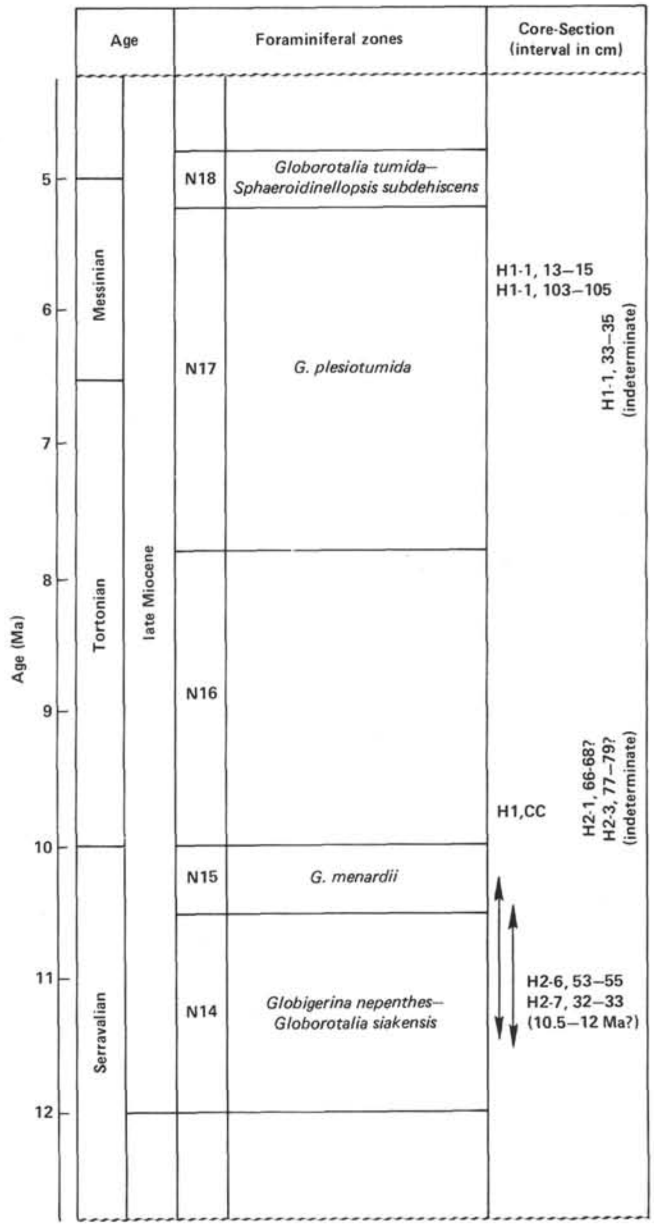

Figure 5. Biostratigraphic zonation of foraminifer samples, Hole 557.

IGNEOUS PETROLOGY AND GEOCHEMISTRY

The first basaltic sample that was incorporated in sediment was retrieved from wash Core H1. The pebble (6 cm in diameter) is a highly vesicular dark gray aphyric basalt.

Only the uppermost 3 m of the basement were drilled from 460.5–463.5 m sub-bottom with 50% recovery. The samples appear to be homogeneous and to form a single lithologic unit. It consists of massive, relatively coarse-grained aphyric basalt, which appears very fresh. The uniformly dark gray color of this basalt may be due to a high content of mafic minerals. Plagioclase laths 2 mm in length are common, and irregular dark patches up to 1 mm can be observed. Vesicules are scattered throughout the section, varying in size from 1 to 3 mm. At 461 m, some large eye-shaped (greater than 1.5 cm) vesicles showing fine-grained geopetal segregation occur. The walls of the vesicles are coated by a black botryoidal mineral. Some of the smaller vesicles are completely filled with glassy segregation material. Clay and calcitic filling of some of the vesicles is due to alteration.

The pebble in the wash Core H1 displays microlithic areas composed of plagioclase and clinopyroxene; these minerals surround the unfilled vesicles (30%) in a halo. Sparse plagioclase microphenocrysts (0.8–1.7 mm) of composition An_{54} (optically determined) are surrounded by plagioclase laths (25%; 0.2–0.6 mm), prismatic clinopyroxene (20%; 0.2–0.6 mm), equant magnetite (5%; 0.1–0.2 mm), and acicular to skeletal ilmenite (4%; 0.2–0.6 mm). Mesostasis (15%) fills the crystal interstices.

The petrographic unit recovered in the uppermost part of the basement (Section 557-1-1) consists of a fresh medium-grained aphyric basalt with intersertal to intergranular texture. Clinopyroxene (35%; 0.1–0.6 mm) occurs as single granules and aggregates up to 1 mm, and, along with devitrified glass[3] (occasionally fresh) (17%), fills the interstices in a random network of larger plagioclase laths (0.4–1.9 mm) with an optically determined composition of An_{56}[4]. Equant magnetite (9%, 0.1–0.5 mm) crystals occur throughout the rock. A series of elongated segregation vesicules filled with devitrified glass lie within a band of small plagioclase (0.1–0.6 mm) and clinopyroxene (0.1–0.6 mm) laths. Devitrified glass, apatite, and magnetite fill the interstices of the laths in this band.

Four samples have been analyzed for major and trace elements, one from the pebble found within the wash Core H1 and three from the basement. The data are reported in Table 3. The composition of the pebble from H1 is very similar in composition to the basement samples. Characteristics of these samples are the high TiO_2 (about 3.5%) and Fe_2O_3 (about 16%) contents and the low MgO value (about 5%), which lead to a very low Mg′ number (about 42%). These features are representative of evolved samples in terms of low-pressure fractional crystallization of olivine and plagioclase and allow the classification of these rocks as ferro basalts.

Chondrite-normalized values of elements Nb, Zr, Ti, Y, and V, which yield plots similar to chondrite-normalized rare earth element (REE) diagrams, show an enriched composition (Fig. 6). The three basement samples analyzed are identical, but the pebble recovered in the sediment is somewhat different, slightly more enriched in the most magmaphile element (Nb). These patterns are similar to those encountered in or near the triple junction area. The absence of a negative Ti anomaly suggests that no removal of titanomagnetite has occurred during the petrogenesis of these basalts.

[3] Onshore microprobe analyses indicate a smectite composition.

[4] Onshore microprobe analyses indicate plagioclase core compositions of An_{59} and rim compositions of An_{48}.

MAGNETICS

Basalt Paleomagnetism

The intensity of NRM was measured for three basalt samples. These samples are more strongly magnetized than those of Site 556. The NRM and susceptibility values are given in Table 4. The high values of susceptibility were believed to be caused by the higher amounts of titanomagnetite in these basalts. This conclusion is supported by the geochemical analyses (see Igneous Petrology and Geochemistry section), which showed higher amounts of titanium in these basalts.

The inclinations are shallower than the expected value of 58° for the dipole magnetic field at the latitude of this site. This may be the result of tectonic rotation.

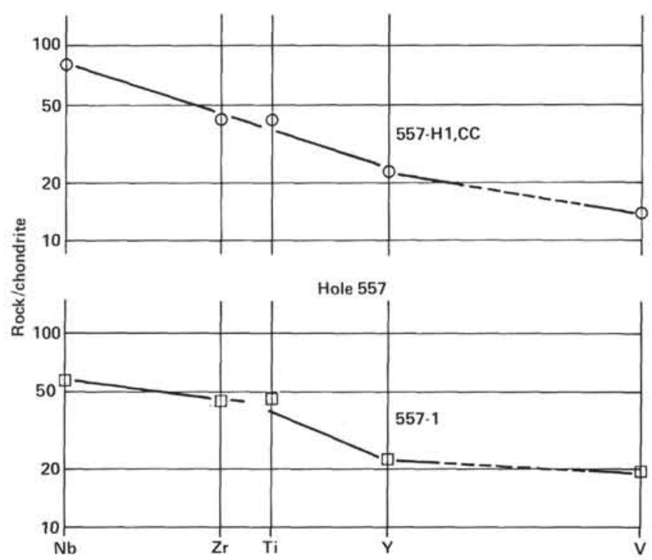

Figure 6. Extended Coryell-Masuda diagrams for Hole 557 basalts.

Table 3. Analyses of major elements (in wt.%) and trace elements (in ppm) for Hole 557 basalts.[a]

Core-Section (interval in cm; piece number)	Depth (m)	Chemical group	SiO_2	TiO_2	Al_2O_3	Fe_2O_3[b]	MnO	MgO	CaO	K_2O	P_2O_5	Total	Mg′[c]	Ti	V	Sr	Y	Zr	Nb
H1,CC		I	49.07	3.28	13.42	15.42	0.18	4.71	9.51	0.61	0.46	96.66	41	19,680	313	344	49.2	219	42.9
1-1, 0–3 (1)	460.5		48.69	3.52	12.53	16.00	0.19	5.92	9.07	0.40	0.38	96.70	45	21,120	415	311	46.7	219	30.2
1-1, 25–28 (3)	460.8		48.22	3.53	12.35	16.79	0.20	5.62	9.73	0.46	0.40	97.30	43	21,180	459	315	48.7	222	29.9
1-1, 40–43 (4)	460.9		48.30	3.49	12.33	16.50	0.23	5.21	10.09	0.45	0.42	97.02	42	20,940	422	300	48.9	220	29.9

[a] On-board measurements were made on ignited samples. Onshore analyses of loss of ignition are less than 1% in most cases. Compiled data tables in Appendix at the end of this volume include volatile components.
[b] Total Fe as Fe_2O_3.
[c] Mg′ is the atomic ratio of $100 \times Mg/(Mg + Fe^{2+})$; calculated using an assumed Fe_2O_3/FeO ratio of 0.15.

Table 4. Magnetic measurements, Hole 557.

Measurement	Core-Section (interval in cm)		
	1-1, 35-37	1-1, 63-65	1-1, 131-133
NRM intensity ($\times 10^{-3}$ emu/cm^3)	3.06	7.02	8.39
χ ($\times 10^{-6}$ emu/cm^3 Oe)	940	700	1110
NRM inclination (°)	44.7	32.7	46.1
Q (= NRM/0.45 χ)	7.23	22.28	16.80

Note: NRM = natural remanent magnetization; Q = Königsberger ratio; χ = susceptibility.

PHYSICAL PROPERTIES

Because of the operational constraints on this hole, only two wash cores were recovered from the sedimentary section. The first contained little undisturbed sediment and was not sampled. The second (from the interval 425.5–460.5 m sub-bottom depth) contained well-lithified sediments from which samples were taken for seismic velocity and density measurements as shown in Table 5.

The sediments recovered are a cyclic sequence, and the base of each cycle is a dark green black color grading to pale gray. In general, the dark bases of cycles are less dense and of lower sonic velocity than the tops, although there does seem to be considerable variability. The very low density and velocity measured on Sample 557-H2-4, 53–61 cm may be due to the presence of burrows within the sample. There seems to be a slight seismic anisotropy within the sediments; *p*-wave velocities parallel to bedding are about 5% greater than vertical velocities.

The high seismic velocity of these sediments contrasts strongly with the sediments encountered at Site 556, where the sediments had a smooth increase in velocity with depth to values of 2.1 km/s at the basement interface. From the reflection profile, the sediment two-way time at Site 557 is 0.38 s, with a prominent reflector at 0.27 s. The total drilled thickness of sediments was 460 m giving a mean velocity of 2.42 km/s. Even if we assume that the strong reflector marks an increase in velocity to 2.60 km/s, the upper sediments would still require a mean velocity of 2.30 km/s. This shows that the whole sedimentary sequence at Site 577 is of higher velocity than that at Site 556 and suggests that the lithologies are correspondingly different.

The quantity of basalt rock recovered in Core 1 was small and no physical properties measurements were made.

SUMMARY AND CONCLUSIONS

Site 557 is located on Magnetic Anomaly 5D (18 Ma old) in the center of a broad (40-km wide) elevated basin (Fig. 7) on the same flow line as Site 556 (34 Ma old) passing through the Azores Triple Junction area. Site 557 is roughly on the same isochron as Site 335, drilled during Leg 37, on a flow line passing through the FAMOUS area (Fig. 7).

Site 557 was located in the center of this basin to avoid elevated ridges and seamounts whose material is generally enriched in the most magmaphile elements. If we had chosen the site on one of the anomalously high features in the area, the finding of "enriched" material could have been attributed to a local event rather than to an event affecting the entire area.

After the sediment was washed down, basement was reached at a sub-bottom depth of 460.5 m. Only the uppermost 3 m of basement were cored because of the rapid approach of a hurricane. A total of 1.2 m of basalt was recovered. An additional basaltic fragment was also collected in a wash core (at 425 m depth). All of the samples recovered are fresh and are characterized by high Fe_2O_3 (16%) and TiO_2 (3.5%) content. The normalized concentrations of magmaphile elements are typical of "light rare earth" enriched material; the normalized concentrations of Nb (same behavior as La) are up to 80 times the chondrite value.

The geochemical data from Sites 556 and 557, together with those of dredged material in the area of the Azores Triple Junction, provide for the first time temporal limits on the behavior of a mantle plume associated with a triple junction. The extended Coryell Masuda plots (using Nb, Zr, Ti, Y and V) shown in Figures 6, 8, and 9 document a clear boundary between the typically de-

Table 5. Physical property measurements, Hole 557.

Core-Section (interval in cm)	Sonic velocity (km/s)			GRAPE density (g/cm^3)		Acoustic impedance ($\times 10^5$) (g/[cm·s])	Lithology
	Vertical	Horizontal	T(°C)	Vertical	Horizontal		
H2-1, 10–13	2.69		21.5	2.20		5.92	Pale gray turbidite
H2-1, 29–33	2.30		21.0	1.94		4.46	Dark gray, basal turbidite
H2-1, 113–119	2.69	2.59	21.0	2.17	2.20	5.70	Pale gray, well-laminated turbidite
H2-2, 54–60	2.59	2.50	21.0	1.91	1.91	4.78	Black massive basal turbidite
H2-4, 53–61	1.88	1.76	21.0	1.80	1.79	3.24	Black burrowed basal turbidite

Note: Sub-bottom depth interval for these samples is 425.5–460.5 m. T = temperature. All values are measured at laboratory temperature and pressure. For details of techniques see Explanatory Notes chapter, this volume.

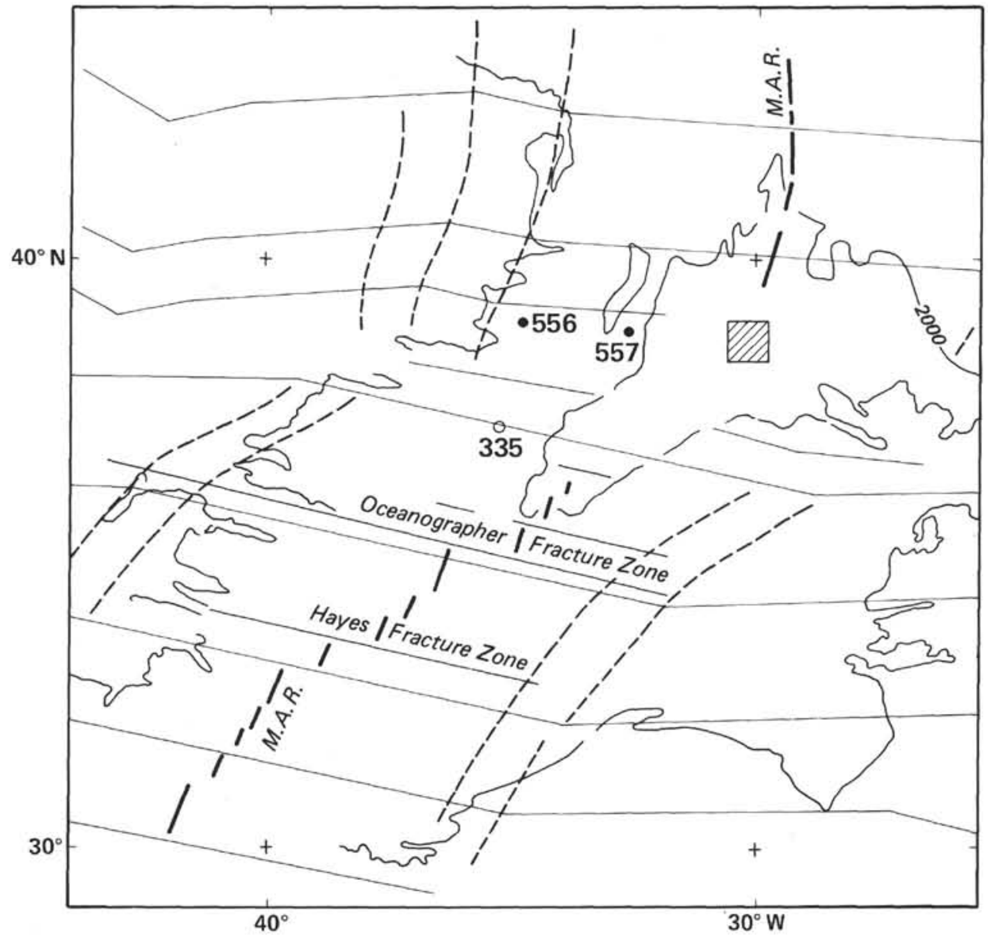

Figure 7. Sketch map of the ocean floor in the vicinity of the Azores Triple Junction. The hachured area marks the location of dredge sites for samples plotted in Figure 9. Contours in meters; straight lines: flow lines; dashed lines: isochrons; circle labeled 335: reference point for Leg 37 (Hole 335); MAR: Mid-Atlantic Ridge.

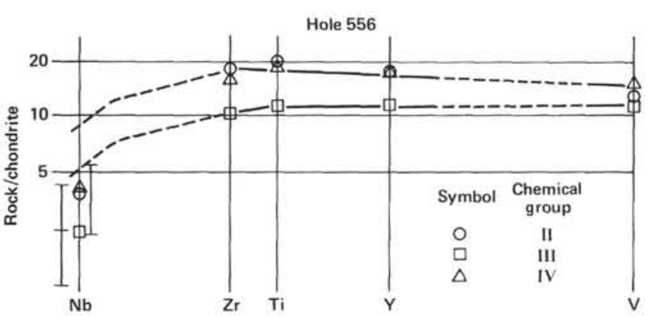

Figure 8. Extended Coryell-Masuda diagram for basalts of chemical Groups II, III, and IV, Hole 556, indicating the depleted character of these rocks. Also shown are error bars for Nb.

pleted oceanic crust at Site 556 (Fig. 8) and the enriched oceanic crust observed both at Site 557 (Fig. 6) and at the triple junction today (Fig. 9).

The geochemical data available do not permit us to locate the actual boundary between basalts with depleted chemical character at Hole 556 (34 Ma old) and basalts with enriched chemical character at Hole 557 (18 Ma old). However, a sharp discontinuity is observed on the seismic profile records in the character of the basement (Fig. 3). The boundary is slightly older than Anomaly 6 (20 Ma) and corresponds to a transition from smooth elevated basement to the east to a more irregular and a more "typical-looking" oceanic basement to the west. We speculate that this topographic boundary corresponds to the geochemical boundary between enriched and depleted oceanic crust.

REFERENCES

Aumento, F., Melson, M. G., et al., 1977. *Init. Repts. DSDP*, 37: Washington (U.S. Govt. Printing Office).

Bougault, H., and Treuil, M., 1980. Mid-Atlantic Ridge: zero age geochemical variations between Azores and 22°N. *Nature*, 986:209–212.

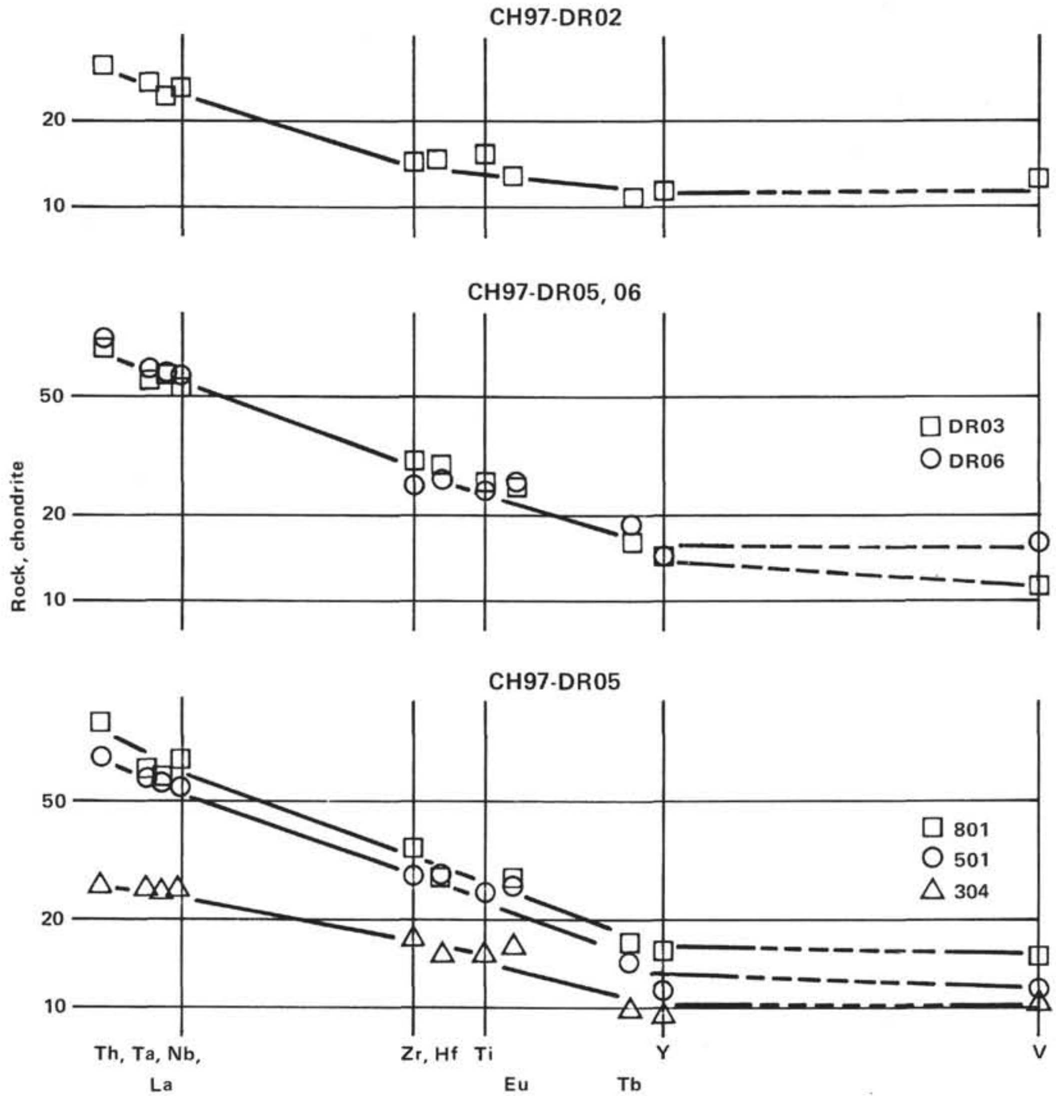

Figure 9. Extended Coryell-Masuda diagrams for samples collected at dredge sites indicated by hachured area in Figure 7. For details, see Bougault and Treuil, 1980.

SITE 557 HOLE CORE H1 CORED INTERVAL 0.0–425.5 m

TIME-ROCK UNIT	BIOSTRATIGRAPHIC ZONE	FOSSIL CHARACTER (FORAMINIFERS, NANNOFOSSILS, RADIOLARIANS, DIATOMS)	SECTION	METERS	GRAPHIC LITHOLOGY	DRILLING DISTURBANCE / SEDIMENTARY STRUCTURES / SAMPLES
upper Miocene	late Miocene N17 (F); N16 (late Miocene) N16 (lower part) (F)		1, 2, CC	0.5, 1.0		

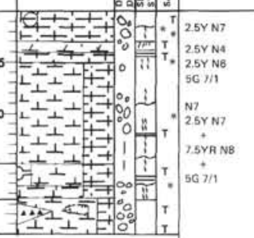

LITHOLOGIC DESCRIPTION

DOMINANT LITHOLOGY NANNOFOSSIL CHALK TO LIMESTONE AND FORAM-NANNOFOSSIL CHALK

(Wash core).

Light gray to greenish gray with darker shades in more siliceous bands.

Parallel and wavy microlaminae: *possible* cross-laminae; *much* bioturbation.

Foram content and size varies to indicate possible micro- or mini-grading: forams in layers grading from larger to smaller, and from less abundant to more abundant, with some layers a foram ooze. Foram content 10–50% (thin section), nannos to 75%.

Minor lithologies:

(1) Basalt: "volcanic bomb(?)" clast of fresh vesicular basalt embedded in sediment in CC; has caused deformation and chertification of underlying sediment layers.

(2) Chert: fragment; dark gray; faint parallel bedding and ripples; abundant silicified forams and minor CO_3 content and (argillaceous limestone on edges).

(3) Nodular limestone: light gray with wavy black streaks and hard lumpy nodules, encrusting. Has high strontium content by XRF analysis.

(4) Siliceous nanno chalk

SMEAR SLIDE SUMMARY (%):

	1-21 D	1-28 M	1-50 D	1-104 M	2-25 D
Composition:					
Feldspar	1	1	Tr	1	Tr
Heavy minerals	Tr	Tr	Tr	Tr	–
Volcanic glass lith. frag.	–	10	Tr	–	–
Pyrite opaques	1	Tr	Tr	1	Tr
Carbonate unspec.	–	Tr	–	–	–
Foraminifers	4	79	25	5	40
Calc. nannofossils	25	–	5	1	5
Diatoms	70	10	70	75	55
Radiolarians	–	–	–	10	–
Sponge spicules	–	–	–	5	–

SITE 557 HOLE CORE H2 CORED INTERVAL 425.5–460.5 m

TIME-ROCK UNIT	BIOSTRATIGRAPHIC ZONE	FOSSIL CHARACTER (FORAMINIFERS, NANNOFOSSILS, RADIOLARIANS, DIATOMS)	SECTION	METERS	GRAPHIC LITHOLOGY	DRILLING DISTURBANCE / SEDIMENTARY STRUCTURES / SAMPLES
upper Miocene	N15/N14 (early late Miocene)		1, 2, 3, 4, 5, 6, 7, CC	0.5, 1.0		

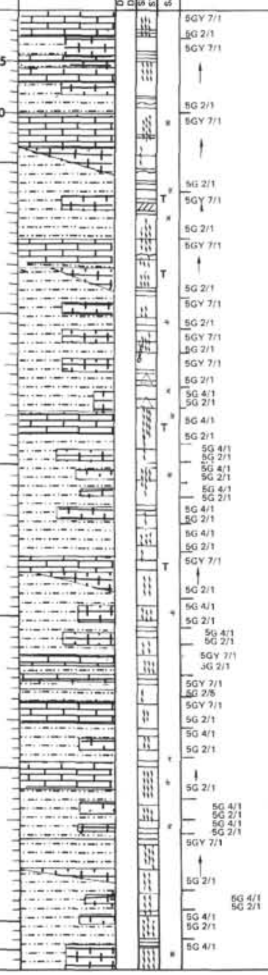

LITHOLOGIC DESCRIPTION

DOMINANT LITHOLOGIES (wash core):

(1) LIMESTONE TO NANNOFOSSIL LIMESTONE TO NANNO-FORAM OR FORAM-NANNO LIMESTONE

Light gray to light greenish gray, grading downward to greenish gray; sharp contacts with overlying black beds.

Intensely bioturbated; bioturbation increasing upward and sometimes abruptly truncated at top at contact with black bed. Few bedding planes.

Nannofossils abundant; forams appear to be more common in more greenish portions; 50–75% of the carbonate may be micrite. Minor constituents are volcaniclastic rock and mineral particles to 2%.

(2) VOLCANICLASTIC NANNOFOSSIL CHALK

Greenish gray, grading upward to light-colored limestone downward to dark-colored mudstone

Intense bioturbation and burrowing; some parallel and wavy bedding, and color-banding

Silt-size particles 10–20%, nannofossils 30–60%, forams 5–10%, volcaniclastic (glass and lithic fragments and clay) 10–25%, and CO_3 20–40%.

(3) CALCAREOUS VOLCANICLASTIC MUDSTONE

Dark greenish gray to black, grading downward from lighter to darker. Sharp contact at base of dark with light gray limestone beneath.

Parallel and wavy bedding, lamination, microcross-laminae; graded beds in fining-upward sequence. Bioturbation intense in darker portions, increasing upward into lighter portions.

Silt-size particles 20–40%, nannofossils 10–15%, forams 3–10%, unspecified carbonate 1–15%, and volcaniclastic (glass, lithic fragments and clay) 40–60%.

SMEAR SLIDE SUMMARY (%):

Lithology type	(1)	(2)	(3)
Composition:			
Feldspar	Tr–1	0–1	Tr–1
Heavy minerals	Tr–1	1–3	1–2
Clay	–	3–5	5–25
Volcanic glass	Tr–2	5–20	40–60
Palagonite	Tr–1	–	Tr–5
Glauconite	–	–	Tr–1
Opaques	Tr–2	Tr	5–15
Micronodules	0–3	1–2	0–2
Zeolite	–	Tr	0–2
Carbonate	50–75	20–40	1–15
Foraminifers	3–8	5–10	3–10
Calc. nannofossils	15–40	30–60	10–15

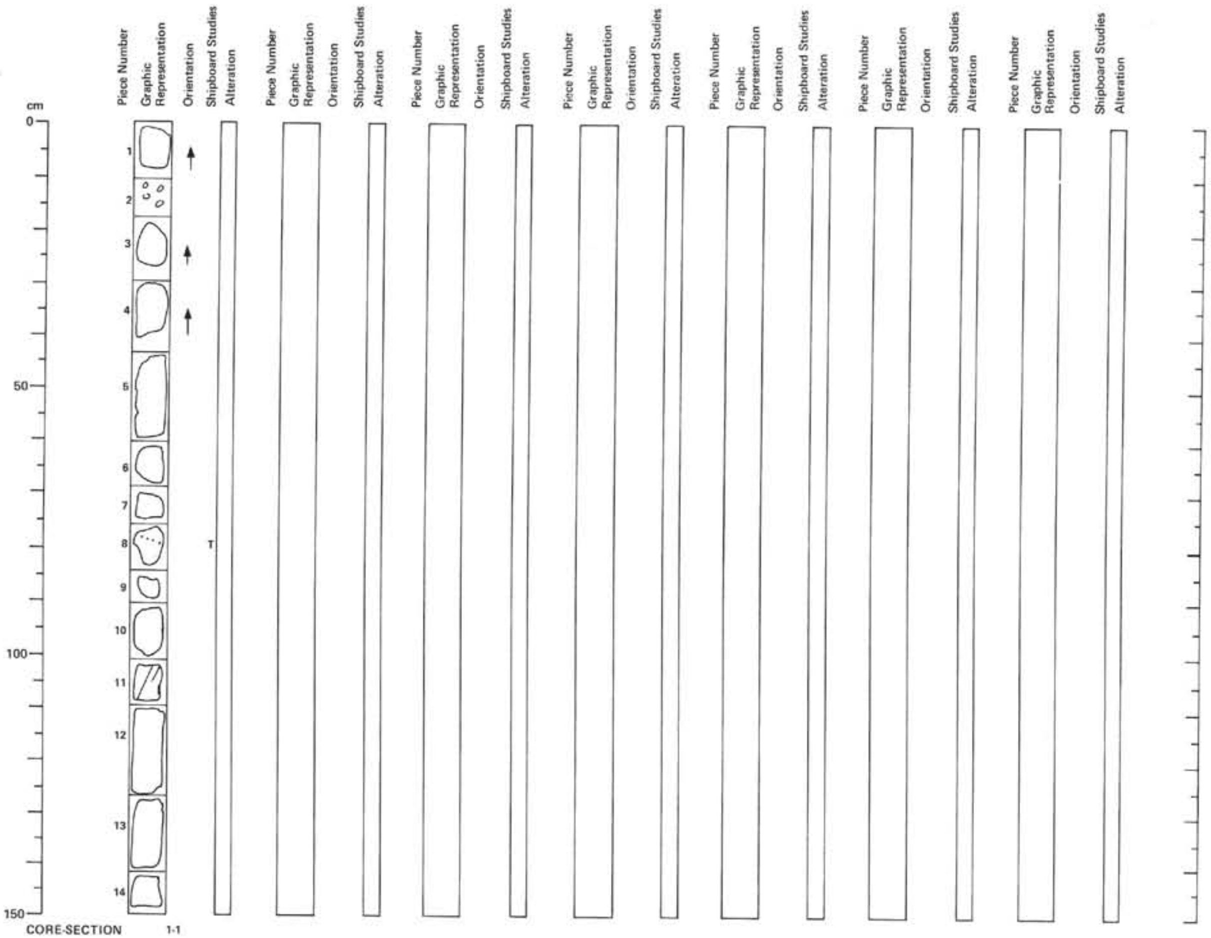

SITE 557, CORE 1 Depth 460.5–463.5 m

SECTION 1

APHYRIC BASALT

Medium-grained aphyric basalt; color dark gray (7.5YR N3/0); appears very fresh except some clay-filled vesicles. Vesicles are mostly round. Their size in the upper third (Pieces 1–5) is between 1 and 3 mm. In Piece 5 some very large segregation vesicles (>1.5 cm) occur. From Piece 6 to the bottom of the section size of vesicles generally decreases to a maximum of ~1.5 mm. Piece 8 shows a group of large vesicles aligned on a plane (shown ⁃ ⁃ ⁃ ......).

Thin Section at 22–25 cm: Medium grained aphyric basalt with intersertal to intergranular texture. Clinopyroxene (35%), and devitrified glass (17%) fill the interstices of randomly placed plagioclase laths (40%). An_{56}. A band of segregation vesicles filled with devitrified glass lie in smaller plagioclase and pyroxene laths.

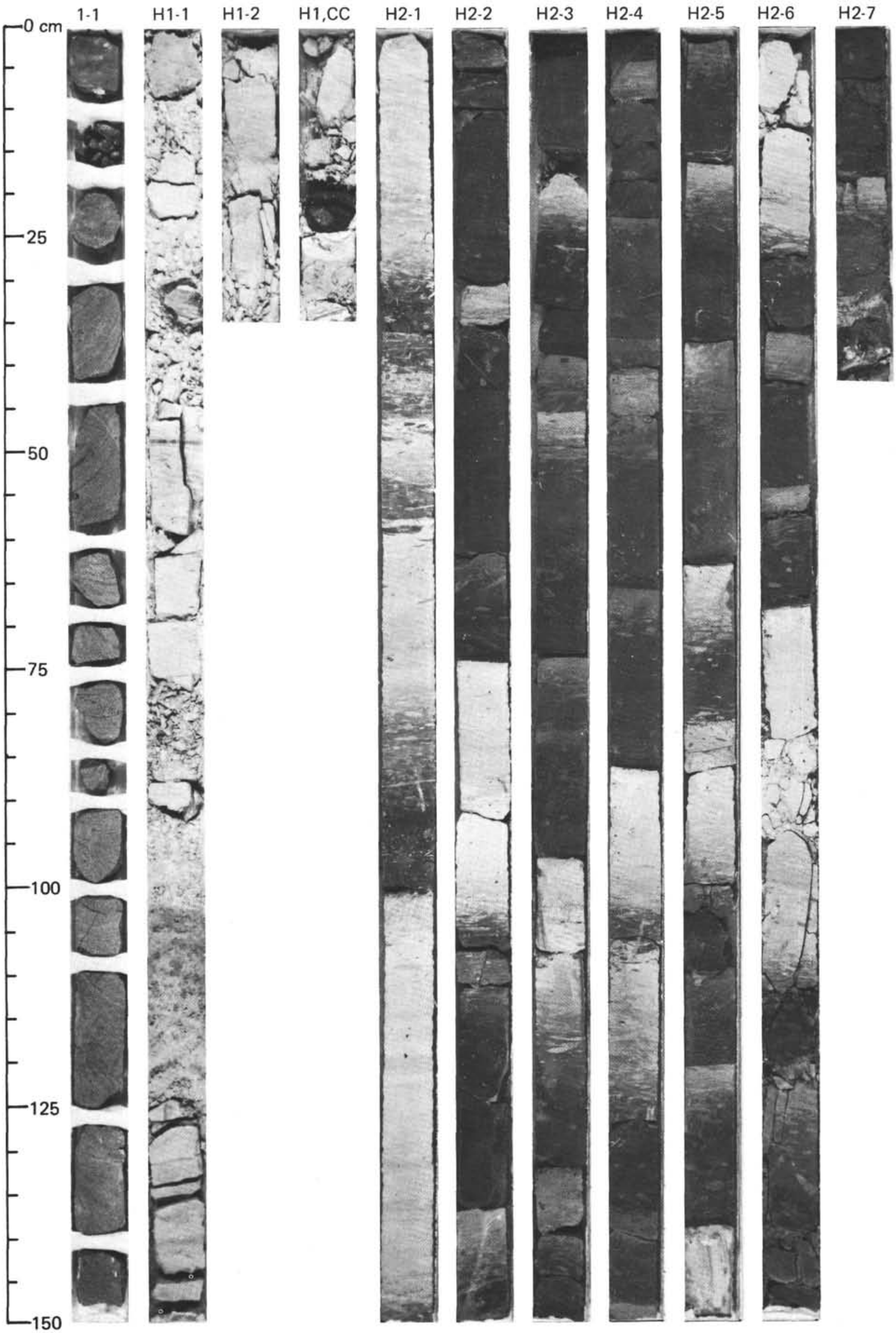
1-1
H1-1
H1-2
H1,CC
H2-1
H2-2
H2-3
H2-4
H2-5
H2-6
H2-7
0 cm
25
50
75
100
125
150